Optics Communications 283 (2010) 2807–2814

Contents lists available at ScienceDirect

Optics Communications

journal homepage: www.elsevier.com/locate/optcom

Operation principle of self-phase compensated optical waveguide isolator

K. Xie [a,*], H.M. Jiang [a], W.Y. Zeng [b], H.J. Yang [c]

[a] School of Optoelectronic Information, UESTC, Chengdu 610054, PR China
[b] Hubei University of Automotive Technology, Shiyan 442002, PR China
[c] School of Physical Electronics, UESTC, Chengdu 610054, PR China

ARTICLE INFO

Article history:
Received 4 November 2009
Received in revised form 21 January 2010
Accepted 4 March 2010

Keywords:
Magnetooptic devices
Magnetooptic isolators
Nonreciprocal wave propagation
Phase matching

ABSTRACT

A theory is developed for the self-phase compensated optical waveguide isolator recently reported in the literature. The operation principle of such device is explained in terms of synchronization of phase and power conversion. The effect of balancing phase mismatches of the two convertors on achieving a proper percentage of mode conversion is revealed. The way to make use of the phase mismatches of different sections to accommodate the different requirements in phase relationship for the reciprocal and nonreciprocal mode convertors is discussed. The theory is extended to the case where phase compensator is used. It is demonstrated that the introduction of phase compensator separates the adjustment of phase from the adjustment of power for the mode convertors so that relaxes fabrication tolerances of such devices. An isolator consists of three phase mismatched waveguide sections is designed and simulated. The simulation results confirm the self-phase compensation theory.

1. Introduction

In optical communication, scattered wave in the guide has influence on the operation of active devices such as semi-conduct laser or optical amplifier, and consequently, the performance of the system could be affected. Optical isolator is a device to suppress such effect so that to improve the stability of the system. Optical circulator is used in splitting and recombining different transmission routes. These devices are commercially available as bulk micro-optical components in the market. It is beneficial to integrate optical components such as light sources, isolators, circulators, modulators, amplifiers and couplers etc. on a single chip in many applications. To alleviate the integration problem, the development of integrated waveguide isolators and modulators for use in such applications is important [1–6].

In the investigation for such integrated, compact devices, several schemes were proposed. The first concept of waveguide isolator is based on nonreciprocal TE-TM mode conversion [7,8]. The nonreciprocal Faraday rotation of magnetooptical materials is the basis of such device. When adapting to waveguide optics, the planar format of guiding structure breaks the symmetry of bulk optical devices. Invariably this leads to a structurally induced birefringence and, consequently, a phase mismatch between TE and TM modes arises.

The main problem in the design of such waveguide isolator is the phase mismatch. It was believed that phase matching has to be adjusted very precisely so that the required isolation can be achieved. Numerous attempts have been made to solve this problem [9–15]. Full phase match has been demonstrated possible by Wolfe et al. [11]. However, quite complicated manufacturing processes are involved in the preparing of the waveguide. The tolerances in the manufacturing make it impractically difficult to achieve the required control of each component of the birefringence. A quasi phase matching solution was proposed by Hutchings [2] as an alternative. But it is noted in the literature that a small relaxation like this in the phase-matching criteria is insufficient.

The enormous difficulties of achieving precise phase matching have led to the investigation of other isolator concepts, including those based on nonreciprocal Mach–Zender interferometer [16,17], on nonreciprocal couplers [18], on nonreciprocal multimode imaging [19,20], and on nonreciprocal amplification [21], etc. However, none of the multitude of prior attempts has so far been translated into a marketable technology, in spite of the strong technological need for on-chip optical isolators.

A scheme that could withstand birefringence is always desirable. The first waveguide isolator technology operating in the presence of phase mismatch was proposed by Dammann et al. [12]. However, in that scheme the through direction is not properly taken care of. The wave passing the first polarizer and the magnetooptic waveguide in the through direction is elliptically polarized. Thus the wave can only partially pass the second polarizer and an intrinsic insertion loss is resulted. In addition to that, the two polarizers are oriented at an angle of 45° with each other, with neither of them pointing in the direction of the waveguide's main axis. Dammann's scheme is therefore difficult to implement in the format of integrated devices.

Recently, a new scheme that could operate in the presence of phase mismatch with better performance and easier manufacturing than Dammann's scheme was reported [23]. It was demonstrated that the

* Corresponding author.
E-mail address: kangxie@uestc.edu.cn (K. Xie).

0030-4018/$ – see front matter © 2010 Elsevier B.V. All rights reserved.
doi:10.1016/j.optcom.2010.03.010

troublesome phase-matching condition for the TE-TM mode conversion could be got rid of without any degradation on the performances of the isolator. The main features of the scheme include the balance between the phase-mismatches of the reciprocal and the nonreciprocal mode convertors, and the redirecting of the effects of phase-mismatches to the creation of a phase jump, which is essential in accommodating the different phase requirements of the two different convertors. The phase matching requirement for each individual mode convertor becomes unnecessary. The use of this scheme enables a waveguide isolator to be built from the principle of Faraday rotation in the presence of phase mismatch. It overcomes the problem of phase mismatch without any complication to the system, so that simplifies the construction of waveguide isolator of this type significantly.

In this work, a theory for the self-phase compensated isolator reported in [23] is developed. The evolution of amplitudes and phases of the TE and TM modes in different sections of the isolator is analyzed. The effect of birefringence on mode power conversion is revealed. The way to make use of the phase mismatch of the guide to adjust the phase relationship between the two modes to suit the different requirements of the two convertors is discussed. Furthermore, an extension of the self-phase compensation scheme is proposed for the use of phase compensator in such isolator. The phase compensator provides a fine tuning on the phase so that the adjustment of phase relationship could be separated from the adjustment of power relationship for the convertors, therefore relaxes the tolerance of manufacturing of such devices. In the presence of phase mismatches, the phase compensator would be shortened because the phase mismatches of the two convertors also have contribution towards the phase adjustment. An isolator consists of a reciprocal convertor, a nonreciprocal convertor, and a phase compensator is designed and simulated. An insertion loss of −0.157 dB and an isolation of −32.1 dB are obtained.

2. The coupled mode theory

For linear, continuous, homogeneous media, Maxwell's equations for time-harmonic waves, of the form $\exp(j\omega t)$ are

$$\nabla \times E = -j\omega\mu_0 H \tag{1}$$

$$\nabla \times H = j\omega\varepsilon_0[\varepsilon]E \tag{2}$$

where ε_0 and μ_0 are the, respective, permittivity and permeability of free space, E is the electric vector, H is the magnetic vector and D is the displacement vector. For a magneto-optical material, $[\varepsilon]$ is the relative permittivity tensor

$$[\varepsilon] = \begin{bmatrix} \varepsilon_{xx} & \varepsilon_{xy} & \varepsilon_{xz} \\ \varepsilon_{yx} & \varepsilon_{yy} & \varepsilon_{yz} \\ \varepsilon_{zx} & \varepsilon_{zy} & \varepsilon_{zz} \end{bmatrix} \tag{3}$$

In this paper, the investigation concerns the longitudinal configuration in which the magnetization points along the propagation direction. For this case, $\varepsilon_{xx} \approx \varepsilon_{yy} \approx \varepsilon_{zz} \equiv \varepsilon_r$, $\varepsilon_{xz} = \varepsilon_{zx} = \varepsilon_{yz} = \varepsilon_{zy} = 0$, $\varepsilon_{xy} = -\varepsilon_{yx} = j\varepsilon_r Q$, where Q is the saturation magnetooptic coefficient induced by the externally applied magnetic field. If the refractive index varies slowly along z, the approximation $\partial\varepsilon_r/\partial z \approx 0$ can be used and the x and y components E_x E_y then become decoupled from the z-component E_z. After these considerations and some lengthy manipulations, we get the wave equation for the principal electric field components E_x and E_y:

$$\begin{aligned} &\frac{\partial}{\partial x}\left(\frac{1}{\varepsilon_r}\frac{\partial(\varepsilon_r E_x)}{\partial x}\right) + \frac{\partial^2 E_x}{\partial y^2} + \frac{\partial^2 E_x}{\partial z^2} + \varepsilon_r k_0^2 E_x + \frac{\partial}{\partial x}\left(\frac{1}{\varepsilon_r}\frac{\partial \varepsilon_r}{\partial y}E_y\right) + j\varepsilon_r Q k_0^2 E_y = 0 \\ &\frac{\partial^2 E_y}{\partial x^2} + \frac{\partial}{\partial y}\left(\frac{1}{\varepsilon_r}\frac{\partial\left(\varepsilon_r E_y\right)}{\partial y}\right) + \frac{\partial^2 E_y}{\partial z^2} + \varepsilon_r k_0^2 E_y + \frac{\partial}{\partial y}\left(\frac{1}{\varepsilon_r}\frac{\partial \varepsilon_r}{\partial x}E_x\right) - j\varepsilon_r Q k_0^2 E_x = 0 \end{aligned} \tag{4}$$

In order to reveal the mechanism underpinning the finding of [23], we turn to the perturbation theory for the development of an analytical description for the operation of the isolator. The terms $\frac{\partial}{\partial x}\left(\frac{1}{\varepsilon_r}\frac{\partial \varepsilon_r}{\partial y}E_y\right)$ and $\frac{\partial}{\partial y}\left(\frac{1}{\varepsilon_r}\frac{\partial \varepsilon_r}{\partial x}E_x\right)$ account for polarization coupling due to geometric effects, the terms $j\varepsilon_r Q k_0^2 E_y$ and $j\varepsilon_r Q k_0^2 E_x$ account for polarization coupling due to magnetooptic effects. In the unperturbed situation the waveguide supports stationary, uncoupled modes. Furthermore, for weakly guiding, the uncoupled modes of the waveguide can be classified into categories of quasi-TE and quasi-TM modes. Suppose that the waveguide cross-section is in the x–y plane and that the wave propagates, predominantly, along the z-direction. The field components of the quasi-TE and quasi-TM modes can be expressed as $E_y = \Xi_y(x,y)\exp(-j\beta_{TE}z)$ and $E_x = \Xi_x(x,y)\exp(-j\beta_{TM}z)$, where $\beta_{TE,TM}$ is the corresponding propagation constant, and $\Xi_{x,y}(x,y)$ is the eigenmode of the waveguide that satisfies Eq. (4) in the absence of the other polarization component.

Suppose the waveguide is cut at corners deliberately, geometric coupling will be introduced into the system. On the other hand, if magnetooptic material is used in the construction of the waveguide, magnetooptic coupling has to be considered. In most cases these coupling terms are so small that they can be treated as perturbations. Eq. (4) can therefore be solved with the first order perturbation method with good accuracy. The stationary solutions $\Xi_{x,y}(x,y)$ are the zeroth order quasi-TM and quasi-TE solutions, and start from which the influence of coupling can be considered. According to the first order perturbation theory, the mode profile $\Xi_{x,y}(x,y)$ and the propagation constant $\beta_{TE,TM}$ will not be affected but the amplitude of the mode is allowed to vary. Ignoring the possibility of coupling to the continuum of radiation modes, and assuming the unperturbed system can only support one single quasi-TE mode and one single quasi-TM mode, then the solution takes the form

$$\begin{aligned} E_x &= A_x(z)\Xi_x(x,y)e^{-j\beta z} \\ E_y &= A_y(z)\Xi_y(x,y)e^{-j\beta z} \end{aligned} \tag{5}$$

where $\beta = (\beta_{TE} + \beta_{TM})/2$. Substitution of Eq. (5) into Eq. (4) leads to

$$2j\beta\frac{\partial A_x}{\partial z}\Xi_x = \frac{\partial}{\partial x}\left(\frac{1}{\varepsilon_r}\frac{\partial \varepsilon_r}{\partial y}\right)A_y\Xi_y + j\varepsilon_r Q k_0^2 A_y\Xi_y - \beta^2 A_x\Xi_x + \beta_{TM}^2 A_x\Xi_x \tag{6a}$$

$$2j\beta\frac{\partial A_y}{\partial z}\Xi_y = \frac{\partial}{\partial y}\left(\frac{1}{\varepsilon_r}\frac{\partial \varepsilon_r}{\partial x}\right)A_x\Xi_x - j\varepsilon_r Q k_0^2 A_x\Xi_x - \beta^2 A_y\Xi_y + \beta_{TE}^2 A_y\Xi_y \tag{6b}$$

The paraxial approximation has been invoked. The power flows along the z direction. It is convenient to define $A_{x,y}$ in such a way that $|A_{x,y}|^2$ corresponds to the power carried by the quasi-TE and quasi-TM modes respectively, which implies that $\frac{1}{2}\frac{\beta}{\mu_0\omega}\int|\Xi_x|^2 dxdy = \frac{1}{2}\frac{\beta}{\mu_0\omega}\int|\Xi_y|^2 dxdy = 1(\text{Watt})$.

Taking the product of Eq. (6a) with $\Xi_x^*(x,y)$ and Eq. (6b) with $\Xi_y^*(x,y)$ for integration from $-\infty$ to $+\infty$. The result is,

$$\begin{aligned} \frac{\partial A_x}{\partial z} &= \kappa_{xy}A_y - j\Delta_\beta A_x \\ \frac{\partial A_y}{\partial z} &= \kappa_{yx}A_x + j\Delta_\beta A_y \end{aligned} \tag{7}$$

where $2\Delta_\beta = \beta_{TM} - \beta_{TE}$ is the phase mismatch between the two polarization components, and

$$\kappa_{xy} = \frac{1}{2\beta\iint|\Xi_x|^2 dxdy}\left[-j\iint\frac{\partial}{\partial x}\left(\frac{1}{\varepsilon_r}\frac{\partial \varepsilon_r}{\partial y}\right)\Xi_x^*\Xi_y dxdy + k_0^2\iint\varepsilon_r Q\Xi_x^*\Xi_y dxdy\right]$$

$$\kappa_{yx} = \frac{1}{2\beta\iint|\Xi_y|^2 dxdy}\left[-j\iint\frac{\partial}{\partial y}\left(\frac{1}{\varepsilon_r}\frac{\partial \varepsilon_r}{\partial x}\right)\Xi_x\Xi_y^* dxdy - k_0^2\iint\varepsilon_r Q\Xi_x\Xi_y^* dxdy\right]$$

are the coupling coefficients. It can be confirmed that the coupling coefficients κ_{xy} and κ_{yx} are related by $\kappa_{xy}=-\kappa_{yx}^{*}=\kappa$. This feature is essential for the conservation of total power.

The general solution of Eq. (7) is

$$\begin{aligned} A_x(z) &= \tau_1 \sin\left(\sqrt{\Delta_\beta^2+|\kappa|^2}z\right)+\tau_2\cos\left(\sqrt{\Delta_\beta^2+|\kappa|^2}z\right) \\ A_y(z) &= \frac{1}{\kappa}\left(\tau_1\sqrt{\Delta_\beta^2+|\kappa|^2}+j\Delta_\beta\tau_2\right)\cos\left(\sqrt{\Delta_\beta^2+|\kappa|^2}z\right) \\ &\quad+\frac{1}{\kappa}\left(j\Delta_\beta\tau_1-\tau_2\sqrt{\Delta_\beta^2+|\kappa|^2}\right)\sin\left(\sqrt{\Delta_\beta^2+|\kappa|^2}z\right) \end{aligned} \tag{8}$$

where the parameters τ_1 and τ_2 are determined from initial conditions. If initial conditions are such that a single mode, say A_x, is incident at $z=0$ on the perturbed region $z>0$, we have $A_x(0)=A_0$, $A_y(0)=0$. Subject to these conditions the parameters τ_1 and τ_2 are obtainable, and the solutions become

$$\begin{aligned} A_x &= \left[\frac{-j\Delta_\beta}{\sqrt{\Delta_\beta^2+|\kappa|^2}}\sin\left(\sqrt{\Delta_\beta^2+|\kappa|^2}z\right)+\cos\left(\sqrt{\Delta_\beta^2+|\kappa|^2}z\right)\right]A_0 \\ A_y &= \frac{-\kappa^*}{\sqrt{\Delta_\beta^2+|\kappa|^2}}\sin\left(\sqrt{\Delta_\beta^2+|\kappa|^2}z\right)A_0 \end{aligned} \tag{9}$$

Power carried in the quasi-TM mode is proportional to $|A_x|^2$, carried in the quasi-TE mode is proportional to $|A_y|^2$. It is seen that power switches forwards and backwards between the two modes periodically. The maximum switchable power is $|\kappa|^2A_0^2/(\Delta_\beta^2+|\kappa|^2)$. In this work a 50% power conversion is required to make the device to work as an isolator, this requires that $|\kappa|\geq|\Delta_\beta|$, i.e., the value $|\Delta_\beta|$ of the phase detuning parameter should not exceed the value $|\kappa|$ of the coupling parameter. The length L of the waveguide for 50% power conversion is given by

$$L=\frac{1}{\sqrt{\Delta_\beta^2+|\kappa|^2}}\arcsin\frac{\sqrt{\Delta_\beta^2+|\kappa|^2}}{\sqrt{2}|\kappa|} \tag{10}$$

It is evident from these expressions that one field component cannot be converted completely into the other field component unless the phase matching condition $\Delta_\beta=0$ is satisfied. Since Δ_β is usually not equal to zero, some means of phase matching has to be used to enhance the TE/TM conversion. In this work a novel phase management scheme is proposed. By this scheme two convertors of different phase mismatches can be joined together by a phase compensator to form a joint-convertor. The phase mismatches for each individual section are somehow compensated with each other, so a 100% TE/TM conversion is achievable without the requirement of phase matching for each individual part.

3. Evolution of waves in the mode convertors

The lengths of the nonreciprocal and the reciprocal mode convertors are taken as their corresponding 50% power conversion lengths, which are respectively denoted as L_{mo} and L_g. For the nonreciprocal convertor, the coupling is due to magnetooptic effect

$$\kappa_{mo}=\frac{1}{2}\varepsilon_r Qk_0^2\iint\Xi_x^{*}\Xi_y dxdy \Big/ \left(\beta\iint|\Xi_x|^2dxdy\right), \tag{11}$$

which is a pure real parameter, with its sign dependent on Q.

Considering the case in which a pure quasi-TM mode is observed at $z=0$. The initial conditions for this case are $A_x(0)=A_0$, $A_y(0)=0$, and the evolution of the wave is described by Eq. (9). At the end of the convertor power is equally distributed between quasi-TE and quasi-TM modes,

$$\begin{aligned} A_x &= \left[\frac{\sqrt{\kappa_{mo}^2-\Delta_{mo}^2}-j\Delta_{mo}}{|\kappa_{mo}|}\right]\frac{A_0}{\sqrt{2}}=\frac{A_0}{\sqrt{2}}e^{j\theta_x} \\ A_y &= -\frac{\kappa_{mo}}{|\kappa_{mo}|}\frac{A_0}{\sqrt{2}}=\frac{A_0}{\sqrt{2}}e^{j\theta_y} \end{aligned} \tag{12}$$

where Δ_{mo} is the modal birefringent parameter of this section. If $Q>0$, the phases at the end of this convertor are $\theta_y=\pi$ and $\theta_x=-\arcsin(\Delta_{\mathrm{mo}}/|\kappa_{\mathrm{mo}}|)$ for the two components, so

$$\phi_{1TM}(+L,Q>0)=\theta_x-\theta_y=-\arcsin\frac{\Delta_{mo}}{\kappa_{mo}}-\pi \tag{13a}$$

The phases at the end of this convertor for the case of $Q<0$ are $\theta_x=-\arcsin(\Delta_{\mathrm{mo}}/|\kappa_{\mathrm{mo}}|)$ and $\theta_y=0$, therefore,

$$\phi_{1TM}(+L,Q<0)=\theta_x-\theta_y=-\arcsin\frac{\Delta_{mo}}{|\kappa_{mo}|} \tag{13b}$$

The phase relationships of this wave at $z=-L_{\mathrm{mo}}$ for $Q>0$ and for $Q<0$ are respectively

$$\phi_{1TM}(-L,Q>0)=\theta_x-\theta_y=\arcsin\frac{\Delta_{mo}}{\kappa_{mo}} \tag{13c}$$

$$\phi_{1TM}(-L,Q<0)=\theta_x-\theta_y=\arcsin\frac{\Delta_{mo}}{|\kappa_{mo}|}-\pi \tag{13d}$$

From these analyses it is understood that if a wave has equal amplitudes of quasi-TE and quasi-TM components and with phase difference of Eq. (13c) for $Q>0$ or Eq. (13d) for $Q<0$, it becomes a pure quasi-TM wave after a propagation distance of L_{mo}. After another propagation distance of L_{mo}, the power is divided equally between quasi-TE and quasi-TM components again, with phase difference of Eqs. (13a) or (13b), depending on the sign of Q.

If the wave appearing at $z=0$ is a pure quasi-TE wave, i.e., $A_x(0)=0$, $A_y(0)=A_0$, the phase relationships of the wave at $z=\pm L_{\mathrm{mo}}$ are obtained as

$$\phi_{1TE}(+L,Q>0)=\theta_x-\theta_y=-\arcsin\frac{\Delta_{mo}}{\kappa_{mo}} \tag{14a}$$

$$\phi_{1TE}(+L,Q<0)=\theta_x-\theta_y=\pi-\arcsin\frac{\Delta_{mo}}{|\kappa_{mo}|} \tag{14b}$$

$$\phi_{1TE}(-L,Q>0)=\theta_x-\theta_y=\pi+\arcsin\frac{\Delta_{mo}}{\kappa_{mo}} \tag{14c}$$

$$\phi_{1TE}(-L,Q<0)=\theta_x-\theta_y=\arcsin\frac{\Delta_{mo}}{|\kappa_{mo}|} \tag{14d}$$

These phase relationships are summarized in Table 1, where $\phi_1=-\arcsin(\Delta_{\mathrm{mo}}/|\kappa_{\mathrm{mo}}|)$. The first figure of the middle line is the phase difference $\theta_x-\theta_y$ of the wave at $z=-0$, while the second figure is the phase difference $\theta_x-\theta_y$ at $z=+0$. At exactly the point $z=0$ a π phase jump occurs while the amplitude for one of the two components drops to zero. Other parts of the table are self-evident.

For the reciprocal convertor, the geometrically induced coupling coefficient is

$$\kappa_g=-\frac{j}{2}\iint\frac{\partial}{\partial x}\left(\frac{1}{\varepsilon_r}\frac{\partial\varepsilon_r}{\partial y}\right)\Xi_x^{*}\Xi_y dxdy\Big/\beta\iint\Xi_x^2dxdy \tag{15}$$

Table 1
Phase relationships between the TE and TM components at $z=0$, $\pm L_{MO}$ for modes that take the form of pure quasi-TM or pure quasi-TE at $z=0$ in magneto optic waveguide.

$\theta_x-\theta_y$	Pure quasi-TM (E_x) at $z=0$		Pure quasi-TE (E_y) at $z=0$	
	$Q>0$	$Q<0$	$Q>0$	$Q<0$
At $z=L_{mo}$	$\phi_1-\pi$	ϕ_1	ϕ_1	$\phi_1+\pi$
At $z=(-0,+0)$	$0,-\pi$	$-\pi, 0$	$\pi, 0$	$0, \pi$
At $z=-L_{mo}$	$-\phi_1$	$-\phi_1-\pi$	$-\phi_1+\pi$	$-\phi_1$

which is a pure imaginary parameter. The sign of κ_g depends on the sign of the integral $\iint \frac{\partial}{\partial x}\left(\frac{1}{\varepsilon_r}\frac{\partial \varepsilon_r}{\partial y}\right)\Xi_x^*\Xi_y dxdy$, which is zero for a rectangular waveguide. If the waveguide is cut at corners, a coupling effect between the E_x and E_y components will be stimulated, geometrically, by the sloping walls. The integral is negative for cuts at the up-left corner or low-right corner so that we have $\kappa_g/|\kappa_g|=j$, while it is positive for cuts at the up-right corner or low-left corner and in this case $\kappa_g/|\kappa_g|=-j$. The phase relationships between the quasi-TE and quasi-TM components for a pure quasi-TE or pure quasi-TM observation at $z=0$ can be found out for the reciprocal convertor in a similar way to that for the nonreciprocal convertor. The results are listed in Table 2, where $\phi_2=-\arcsin(\Delta_g/|\kappa_g|)+\pi/2$ and Δ_g is the modal birefringent parameter of this reciprocal section.

4. Synthesis of waveguide isolator

With these phase relationships in mind, a waveguide isolator can be synthesized by a proper combination of the phase mismatches of the nonreciprocal and reciprocal convertors. The core part of the proposed isolator consists of a nonreciprocal waveguide section of lengths L_{mo}, a reciprocal waveguide section of lengths L_g, and a birefringent waveguide section of length L_b in between. The first and last sections are respectively a nonreciprocal 45° polarization rotator and a reciprocal 45° polarization rotator. The central section is a phase compensator, in which the quasi-TE and quasi-TM waves are not coupled but have different propagation constants so an adjustment on their phase relation results. The three sections are joined with each other in a cascade fashion. Suppose the three waveguide sections have similar cross sections so that reflections at these interfaces are minimized. By adjusting the parameters of each section, the profile of phase relation can be tailored so that the joint-convertor becomes a one way 90° polarization rotator. It achieves a complete TE/TM conversion for waves propagating in one direction, while preserves the input polarization for waves propagating in the opposite direction.

Suppose a pure quasi-TE wave of amplitude A_0 is fed to the nonreciprocal convertor. If the direction of magnetization and direction of propagation are both in the z direction, $Q>0$ arises and the wave amplitudes at the end of this convertor become $|A_x|=|A_y|=A_0/1.414$, with a phase difference of ϕ_1. In the phase compensator the amplitude relation remains the same but, since different phase delays are imposed on the quasi-TE and quasi-TM components, an extra phase difference $\Delta\phi$ is introduced. The phase relation of the two wave components at the end of the phase compensator therefore becomes $\phi_1+\Delta\phi$. For the third section let's assume the geometric coupling of the reciprocal convertor is introduced by up-left/low-right cuts, so that the coupling coefficient is $\kappa_g/|\kappa_g|=j$. It can be derived from Tables 1 and 2 that if the incident quasi-TE and quasi-TM waves at the beginning of the reciprocal rotator are equal in amplitude and have a phase relation of $-\phi_2$, a pure quasi-TE wave emerges after a propagation distance of L_g. By setting the phase relation at the end of the phase compensator to $-\phi_2$, the following condition is established

$$\phi_1+\phi_2+\Delta\phi=0 \tag{16a}$$

which is the condition for the joint-convertor to preserve the input polarization for the forwards propagating wave.

For backwards propagation, the pure quasi-TE incident wave encounters with the reciprocal convertor first. From the wave's point of view, the up-left/low-right cuts of the waveguide now become up-right/low-left cuts for the backwards propagation so $\kappa_g/|\kappa_g|$ changes sign. At the end of this section a mixture of TE-TM wave is delivered, with equal amplitudes and a phase difference of $\phi_2-\pi$. After passing the phase compensator the phase relation becomes $\phi_2+\Delta\phi-\pi$ and according to Eq. (16a), this is equal to $-\phi_1-\pi$. When the wave propagates through the nonreciprocal convertor, since the external magnetization and the wave's way of propagation are now opposite in direction, $Q<0$ is observed. By consulting with Table 1, a pure quasi-TM wave emerges at the end of this section. The input polarization is therefore verified to switch to the other polarization in the case of backwards propagation, which confirms that for the same magnetization and physical cuts the joint-convertor behaviors differently for the backwards propagations from that for the forwards propagation. Similar behavior is observed for a quasi-TM input. The phase-matching requirement for each individual convertor is removed. An optical waveguide isolator can be built based on this principle of operation.

The length of the phase compensator could be changed to other values so that the following condition is observed

$$\phi_1+\phi_2+\Delta\phi=\pm n\pi,\quad (n=0,\ 1,\ 2,\ \cdots) \tag{16b}$$

It is found that in the case of even integer n the joint-convertor performs in the same fashion as that described above. On the other hand, if the integer n is odd the rotations caused by the two convertors add up to produce a desired 90° total rotation of polarization in the forwards direction, while they cancel with each other to give a total rotation of 0° in the backwards direction. So the joint-convertor preserves the polarization of the input wave for backwards propagation and converts it into the other polarization for forwards propagation. Eq. (16b) is a more general condition of operation for the isolator over Eq. (16a).

It can be demonstrated that the isolator reported in [22] is a special case of Eq. (16). For example, for the waves shown in Fig. 4 of [22], the phase differences at the end of the two convertors are respectively $\phi_1=180°$ and $\phi_2=90°$, the extra phase shift introduced by the phase compensator is $\Delta\phi=-90°$, so $\phi_1+\phi_2+\Delta\phi=180°$. For waves shown in Fig. 5 of [22], the phase differences at the end of the two convertors are respectively $\phi_1=0°$ and $\phi_2=-90°$, the extra phase shift introduced by the phase compensator is again $\Delta\phi=-90°$, so $\phi_1+\phi_2+\Delta\phi=-\pi$. In both cases the condition of Eqs. (16a) and (16b) is satisfied. It is noted that for the phase-matched cases, definite phase relation between the quasi-TE and quasi-TM modes is present so a phase compensator has always to be inserted to provide the $\pm 90°$ phase jump. For phase mismatched cases on the other hand, the layout of the device is similar but since neither ϕ_1 nor ϕ_2 is fixed, other values of $\Delta\phi$ are possible. If the combination of ϕ_1 and ϕ_2 produces a value close to $\pm n\pi$, the phase jump $\Delta\phi$ needed from the phase compensator is small so that its length can be reduced. In the special case of $\phi_1+\phi_2=\pm n\pi$, phase compensator can be omitted all together. In this case the situation reduces to that considered in [23]

Table 2
Phase relationships between the TE and TM components at $z=0$, $\pm L_g$ for modes that take the form of pure quasi-TM or pure quasi-TE at $z=0$ in geometric coupling waveguide.

$\theta_x-\theta_y$	Pure quasi-TM (E_x) at $z=0$		Pure quasi-TE (E_y) at $z=0$	
	$\kappa_g/\|\kappa_g\|=j$	$\kappa_g/\|\kappa_g\|=-j$	$\kappa_g/\|\kappa_g\|=j$	$\kappa_g/\|\kappa_g\|=-j$
At $z=L_g$	$\phi_2-\pi$	ϕ_2	ϕ_2	$\phi_2-\pi$
At $z=(-0,+0)$	$\pi/2,-\pi/2$	$-\pi/2,\pi/2$	$-\pi/2,\pi/2$	$\pi/2,-\pi/2$
At $z=-L_g$	$-\phi_2+\pi$	$-\phi_2$	$-\phi_2$	$-\phi_2+\pi$

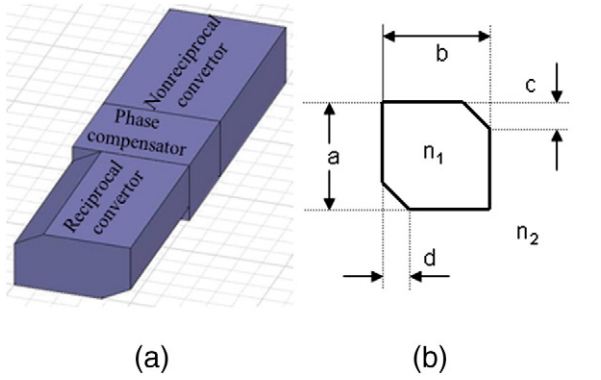

Fig. 1. Configuration of the optical waveguide isolator consisting of three sections. (a) Three dimensional sketch; (b) Cross section of the optical waveguide.

and the operation condition of Eq. (16b) reduces to a form coincides with Eq. (5) of [23] apparently. In this sense the condition proposed by [23] is extended by Eqs. (16a) and (16b) to cover the case where phase compensator is inserted. Since both power and phase have to satisfy certain conditions at the end of the joint-convertor simultaneously for the configuration of [23], the isolator proposed there is somewhat difficult to build. The introduction of phase compensator separates the phase condition from the power condition for the joint-convertor. The difficulty of manufacturing is reduced for the isolator proposed in this work.

5. Numerical simulations

The behavior of the proposed device can be numerically investigated with the full vectorial finite-difference beam propagation method [22], based on the vectorial coupled wave Eq. (4). In this numerical study, each section of the joint-convertor is realized with a buried waveguide of the same type but of different dimensions, as shown in Fig. 1. The material forming the waveguide core is Ce: YIG, and the surrounding substrate is GGG material. The refractive indices of the guiding section and the substrate are, respectively, $n_1=2.09$, $n_2=1.95$. The nonreciprocal convertor is magnetized longitudinally, and the magnetooptical coefficient for the core material is $|Q|=0.87\times10^{-3}$. The rest of the isolator is not magnetized so $Q=0$ for other sections of the device. The choice of parameters a and b are arbitrary, provided that the waveguide supports only a single TE mode and a single TM mode. This is the condition for the device to operate correctly. The values of parameters c and d are also arbitrary to an extent. They are determined by the following concerns. The geometrically induced reciprocal coupling coefficient is dependent of the size of the cuts. A very small c and d results in a too long reciprocal convertor to use conveniently, while a very large c and d may perturb the modes so much that a huge reflection rises at the interfaces between different convertors. In the simulations, the wavelength is assumed to be $\lambda=1.55$ μm, and $a=0.8$ μm, $b=0.9$ μm, $c=d=0$ for the phase compensator and the nonreciprocal convertor. For the reciprocal convertor the parameters a and b are the same, but $c=a/4$ and $d=b/4$ for the cuts. The length of the reciprocal waveguide needed for 45° rotation is found to be 609 μm, with a phase difference of $\phi_2=49.5°$ at the end. The length of the nonreciprocal waveguide required for 45° rotation is found to be 421 μm, with a phase difference of $\phi_1=-30.1°$ at the end. According to Eqs. (16a) and (16b), a phase shift $\Delta\phi=-\phi_1-\phi_2=-19.4°$ has to be introduced for the device to operate correctly. The length of the phase compensator needed for −19.4° phase correction is found to be 175 μm.

The simulated behavior of waves in passing the device in the forwards direction is shown in Fig. 2, where $Q<0$ and $\kappa_g/|\kappa_g|=-j$ are used. The input wave is a quasi-TM mode whose power is normalized to 1 W. The first section of the device is a nonreciprocal convertor. In this section the quasi-TM wave is converted into quasi-TE wave due to the magnetically-induced coupling, so the E_y component grows and the E_x component decreases during propagation. Since the amplitude of the quasi-TE wave is, initially, zero so the phase difference between the quasi-TE and quasi-TM wave is not well-defined in the beginning. After a transition stage the quasi-TE wave generated by this effect is found to be in phase with the quasi-TM parent wave, but they are gradually desynchronized by the waveguide birefringence. At the end of this section, the input quasi-TM wave is damped to −3 dB level, and the generated quasi-TE wave grows up to the level of −3 dB. Half of the input power is converted into quasi-TE component, with a phase difference of $\phi_1=-30.1°$ between the two components. The second section is a phase compensator. The quasi-TE and quasi-TM waves are not coupled in this section but propagate at different phase velocities, so their phase difference changes during propagation. At the end of this section, their phase difference is decreased to $\phi_1+\Delta\phi=-49.5°$, as indicated by the solid curve in Fig. 2(b). The third section is a reciprocal convertor in which the quasi-TE and quasi-TM waves are coupled by geometric effects and the conversion between the quasi-TE and quasi-TM waves starts again. Since $\kappa_g/|\kappa_g|=-j$ in this particular example, the condition $\theta_x-\theta_y=-49.5°=-\phi_2$ implies that a pure quasi-TM wave will appear after a propagation distance of $L_g=608.5$ μm. This indicates that in the reciprocal convertor E_x is being generated by E_y. As the quasi-TE wave is being converted back into quasi-TM wave, the quasi-TE wave is damped to −32.1 dB and the quasi-TM wave grows to −0.157 dB at the end of this section. The polarization of the beam becomes parallel to the x-axis again. From the trend of variation the phase difference is made out approaching $-\pi/2$. However, it becomes uncertain at the end, due to the fact that the quasi-TE wave is at a very low level, reaching the noise floor of the computational calculation. After this point, a π jump in the phase difference is expected, as suggested in Table 2. The two rotations, respectively introduced by the reciprocal convertor and the nonreciprocal convertor, cancel with each other in this configuration. The quasi-TM input is output as a quasi-TM wave, with a quasi-TE wave appearing as intermediate product.

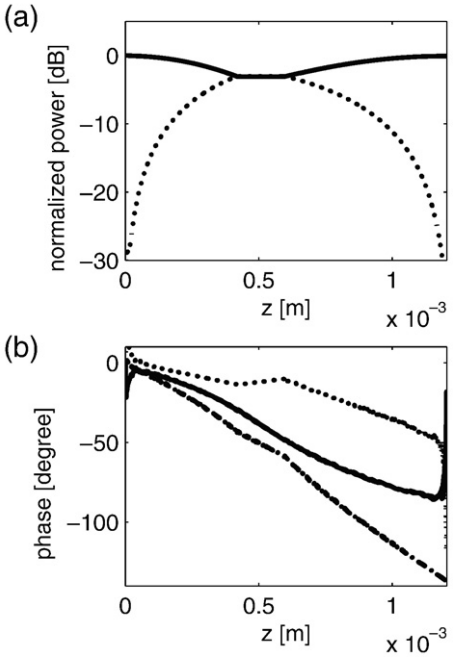

Fig. 2. Evolution of the waves propagating in the forwards direction for $Q>0$. (a) Normalized power (solid curve: quasi-TM wave, dotted curve: quasi-TE wave). (b) Phases (dashed curve: θ_x, dotted curve: θ_y, solid curve: $\phi=\theta_x-\theta_y$).

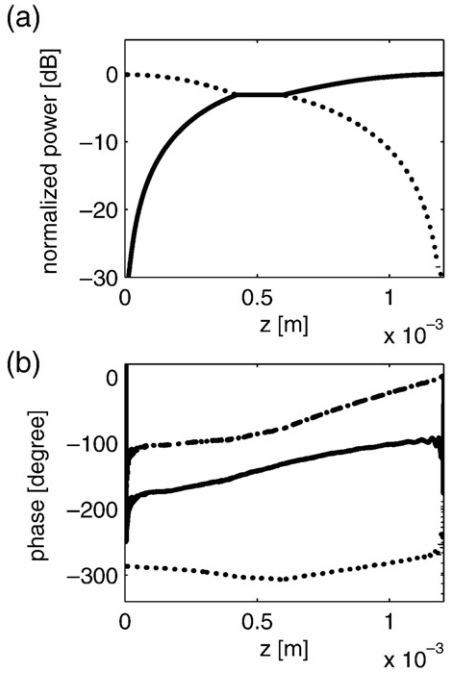

Fig. 3. Evolution of the waves travelling in the backwards direction for $Q<0$. (a) Normalized power (solid curve: quasi-TM wave, dotted curve: quasi-TE wave). (b) Phases (dashed curve: θ_x, dotted curve: θ_y, solid curve: $\phi=\theta_x-\theta_y$).

If both the reciprocal mode convertor and the nonreciprocal mode convertor are individually phase-matched, according to the analysis of [22], the introduction of $-\pi/2$ jump in phase difference is necessary for the power conversion to carry on from the first convertor to the next one. In other words, to prepare the wave from one phase relationship suitable for the nonreciprocal convertor to a different phase relationship suitable for the reciprocal convertor, a phase shift of $-\pi/2$ has to be imposed on the wave at the junction of the two convertors. A phase compensator of length 822 μm was inserted for this purpose in [22]. It is noted from Fig. 2(b) that the span of change in phase difference is $-\pi/2$ for the wave to travel the whole length of the device, which coincides with the phase jump required for a perfectly phase-matched system. But in the current scheme it is revealed that the $-\pi/2$ phase shift is divided between the three sections of the device. Each section contributes a share to the phase jump. The demand for phase correction on the phase compensator is therefore eased and the length of phase compensator is shortened as a consequence. It is seen both the birefringence in the reciprocal convertor and the nonreciprocal convertor contribute to the $-\pi/2$ phase shift. From this study, it is evident that the detrimental phase-mismatches are turned into a useful effect by the phase management scheme. The phase-mismatches are made use of in preparing the wave for the correct phase relationships. In the current configuration, the length of the phase compensator used is 175 μm, which is much shorter than the length of 822 μm that was used in [22] for the phase-matched situation. If enough contribution is collectable from the two convertors for the phase jump, the phase compensator could be omitted altogether.

The simulation results for waves propagating in the backward direction are shown in Fig. 3 for a pure quasi-TM input. The first section the input wave encounters from the back is the reciprocal convertor. From this direction the cuts are at the up-left and low-right corners of the guide, so $\kappa_g/|\kappa_g|=j$ is experienced by the waves. The phase difference between the generated quasi-TE wave and the quasi-TM parent wave oscillates a bit due to the small initial amplitude of the quasi-TE wave. It settles down to $-\pi/2$, and then continuously decreases due to the phase mismatch, to $-130.5^\circ=\phi_2-\pi$ as it reaches the end of the reciprocal convertor. At this point, half of the input power is converted into quasi-TE component. The polarization angle of the input beam is rotated by 45°. The second section is the phase compensator in which the amplitudes of the quasi-TE and quasi-TM waves are maintained but their relative phase is decreasing during propagation. At the end of this section, a phase difference of $-149.4^\circ=\phi_2-\pi+\Delta\phi$ is achieved. The third section is a nonreciprocal convertor. Since the wave now propagates in the same direction as the externally applied magnetic field, $Q>0$ is experienced. According to Table 1, the relative phase between the quasi-TE and quasi-TM waves, which is $\phi_2-\pi+\Delta\phi=-\phi_1-\pi\equiv-\phi_1+\pi$, is suitable for E_x to generate E_y. The wave emerges after a propagation distance of L_{mo} will be a pure quasi-TE mode. A subsequent rotation of polarization is activated and in the end another 45° rotation is completed. The rotations accumulated in the reciprocal and nonreciprocal convertors are found additive in this case. Upon reaching the end of the device a total rotation of 90° in polarization is produced. The direction of polarization is now parallel to the y-axis as almost all power is converted into quasi-TE mode. The phase difference approaches $-\pi$ towards the end but its trace is lost in noise as the amplitude of the quasi-TM wave approaches the noise floor of the computational calculation. If a TM polarizer is attached to the joint-convertor, the TE component would be damped so that only a very weak residual of the TM component would be emitted from the device. An isolation of −32.1 dB is expected.

Since the device consists of several sections, and the eigenmodes of different sections are not exactly matched, there are reflections indeed at the interface between any two sections. These reflections are taken into account in the numerical modeling as scattering losses. It is reflected in the reduction of the total power. The numerical simulation of this example (Figs. 2 and 3) shows that the output power is −0.16 dB lower than the input power. Because the cross sections of the three different parts of the proposed isolator are deliberately designed to support modes of similar profiles, these reflections are so small that no significant influence on the performance of the device is found.

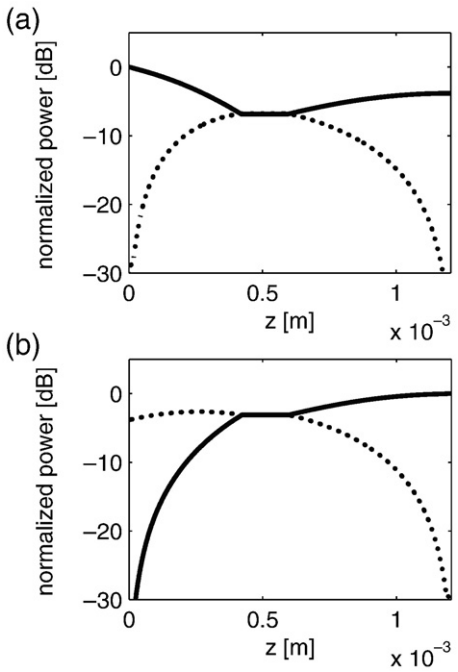

Fig. 4. Evolutions of waves in the presence of material loss for (a) forward propagation and (b) backward propagation (solid curve: quasi-TM wave, dotted curve: quasi-TE wave).

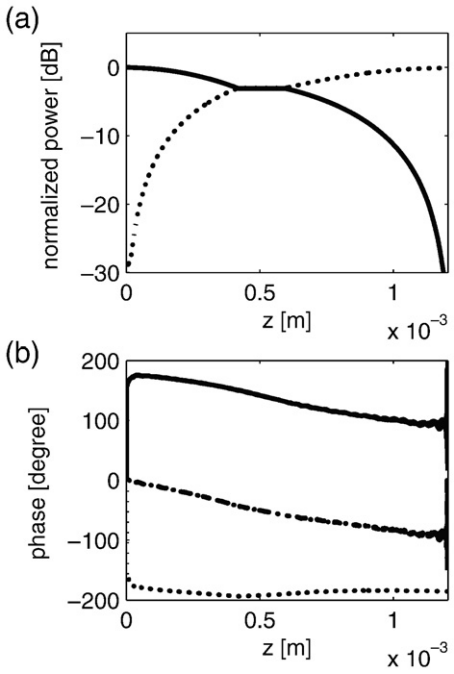

Fig. 5. Evolution of the waves propagating in the forwards direction for $Q<0$. (a) Normalized power (solid curve: quasi-TM wave, dotted curve: quasi-TE wave). (b) Phases (dashed curve: θ_x, dotted curve: θ_y, solid curve: $\phi=\theta_x-\theta_y$).

Since absorption is not weak when dealing with magneto-optical elements, its influence on the operation of the proposed isolator needs to be assessed to get a full picture of the device. Loss is represented by the imaginary part n'' of the refractive index of the material, i.e. $n=n'-in''$. The magneto-optics material Ce: YIG used for the numerical simulations in this work indeed has an imaginary part of refractive index of the order 10^{-4} : $n=2.09-0.000477i$. The evolutions of waves in the presence of material loss are shown in Fig. 4 for both forward and backward propagations. It is seen that absorption does not break the balance of TE and TM components. The conversion distances are compatible with losses. An extra 3.84 dB loss is imposed on both the insertion loss and isolation of the device, but the operation principle of the isolator is preserved.

The same device can be used as an optical modulator by periodically switching the direction of the externally applied magnetic field. The behavior of a forwards travelling quasi-TM input is simulated for the case of oppositely applied magnetic field, and the result is shown in Fig. 5. Comparing with Fig. 2, it is seen that the phase difference between the quasi-TE and quasi-TM waves starts from π instead of 0, due to the reversal of magnetization. As the wave reaches the end of the nonreciprocal convertor, the phase difference becomes $-\phi_2+\pi(=130.5°)$ instead of $-\phi_2(=-49.5°)$. In the reciprocal convertor, since $\kappa_g/|\kappa_g|=-j$ for forwards propagation, by consulting with Table 2, this particular phase difference would activate a process of converting quasi-TM component into quasi-TE component. As expected, the output wave is a pure quasi-TE mode. The phase difference approaches $\pi/2$ at the end. It is evident from the calculations that by reversing the direction of magnetization, the polarization of the output would be exchanged. If a TM polarizer is attached, the power level of the output wave would be preserved for a TM output and be damped for a TE output, and the function of an optical waveguide modulator is then realized.

In order to evaluate the tolerance of the isolator to fabrication error, the length of the phase compensator is deliberately extended by 10% and the resulting isolation is examined. It is found that when the length of the phase compensator increases from 175 μm to 193 μm, the isolation drops from −32.1 dB to −29.99 dB. This indicates that the isolation is not sensitive to phase error. On the other hand, as the length of the nonreciprocal or reciprocal convertor changes, not only a phase error is introduced, but also the balanced 50:50 power splitting between TE and TM modes breaks. The isolator is found more sensitive to amplitude error than phase error. For isolator of fixed nonreciprocal convertor (421 μm long) and fixed phase compensator (175 μm long), the variation of isolation as function of the length of the reciprocal convertor can be read off from Fig. 2a by moving along the z axis from the end ($z=421\,\mu m+175\,\mu m+609\,\mu m$) to where the reciprocal convertor starts ($z=421\,\mu m+175\,\mu m$). At any point z the length of the reciprocal convertor is represented by $z-(421+175)\mu m$. For isolator of fixed reciprocal convertor (609 μm long) and fixed phase compensator (175 μm long), the variation of isolation as function of the length of the nonreciprocal convertor can be read off from Fig. 3a by moving along the z axis from $z=0$ to $z=421\,\mu m$, where $421\,\mu m-z$ represents the length of the nonreciprocal convertor. It can be derived from the two figures that when the convertor reaches the "desired" length, the isolator reaches its peak performance. The performance degrades quickly around the peak, the lengths of the two convertors should therefore be control more precisely than the length of the phase compensator.

6. Summary

The self-phase compensation phenomenon observed in the construction of optical waveguide isolator is explained with the coupled mode theory. This phenomenon was first discovered in [23] via computational modeling. In this study a theory for its mechanism is developed based on the coupled mode equations. In addition, this study extends the self-phase compensation scheme to a more general case where phase compensator is used. By this scheme the usual phase matching requirement for mode convertor is eliminated. A waveguide isolator could be built from phase mismatched waveguide mode convertors. It is worth pointing out that the device proposed in [23], which does not require phase matching in the sections, requires the phase difference between TE and TM to be accurately controlled. This is not necessarily easier than phase matching. It is the use of phase compensator proposed in this work that really relaxes the realization conditions of the self-phase compensation technology. Application of the theory to an optical isolator constructed from longitudinally magnetized three-dimensional magnetooptical waveguide section is discussed. An isolator of this type is designed and simulated using a full-vectorial finite difference beam propagation method. The insertion loss of the isolator is estimated −0.157 dB and the isolation is estimated below −32.1 dB. Many magneto-optical materials are lossy. When material loss is taken into account, the operation principle of the proposed isolator is not destroyed but an extra 3.84 dB loss is imposed on both the insertion loss and isolation of the device. The simulation results confirm the feasibility of the proposed isolator and the self-phase compensation theory.

Acknowledgment

This work was supported in part by NSFC under Grants 60588502 and 60607005.

References

[1] H. Dotsch, N. Bahlmann, O. Zhuromskyy, M. Hammer, L. Wilkens, R. Gerhardt, P. Hertel, J. Opt. Soc. Am. B 22 (2005) 240.
[2] D.C. Hutchings, J. Phys. D 36 (2003) 2222;
B.M. Holmes, D.C. Hutchings, Appl. Phys. Lett. 88 (2006) 061116.
[3] K. Postava, M. Vanwolleghem, D.V. Thourhout, R. Baets, S. Visnovsky, P. Beauvillain, J. Pistora, J. Opt. Soc. Am. B 22 (2005) 261.
[4] V. Zayets, M.C. Debnath, K. Ando, J. Opt. Soc. Am. B 22 (2005) 281.
[5] R.L. Espinola, T. Izuhara, M.C. Tsai, R.M. Osgood Jr., H. Dotsch, Opt. Lett. 29 (2004) 941.
[6] B. Sepulveda, L.M. Lechuga, J. Lightwave Technol. 22 (2004) 1772.

[7] K. Ando, T. Okoshi, N. Koshizuka, Appl. Phys. Lett. 53 (1988) 4.
[8] J.P. Castera, G. Hapner, IEEE Trans. Magn. MAG-13 (1) (1977) 1583.
[9] H. Dammann, E. Pross, G. Rabe, Appl. Phys. Lett. 49 (1986) 1755.
[10] R. Wolfe, V.J. Fratello, M. NcGlashan-Powell, Appl. Phys. Lett. 51 (1987) 1221.
[11] R. Wolfe, V.J. Fratello, M. McGlashan-Powell, J. Appl. Phys. 63 (1988) 3099.
[12] H. Dammann, E. Pross, G. Rabe, W. Tolksdorf, Appl. Phys. Lett. 56 (1990) 1302.
[13] R. Wolfe, J.F. Dillon Jr., R.A. Liebermann, V.J. Fratello, Appl. Phys. Lett. 57 (1990) 960.
[14] T. Shintaku, Appl. Phys. Lett. 73 (1998) 1946.
[15] M. Lohmeyer, N. Bahlmann, O. Zhuromskyy, H. Dotsch, P. Hertel, J. Lightwave Technol. 17 (1999) 2605.
[16] F. Auracher, H.H. Witte, Opt. Commun. 13 (1975) 435.
[17] J. Fujita, M. Levy, R.M. Osgood Jr, L. Wilkens, H. Dotsch, Appl. Phys. Lett. 76 (2000) 2158.
[18] N. Bahlmann, M. Lohmeyer, O. Zhuromskyy, H. Dotsch, P. Hertel, Opt. Commun. 161 (1999) 330.
[19] J.S. Yang, J.W. Roh, S.H. Ok, D.H. Woo, Y.T. Byun, W.Y. Lee, T. Mizumoto, S. Lee, IEEE Trans. Magn. 41 (2005) 3520.
[20] M. Lohmeyer, L. Wilkens, O. Zhuromskyy, H. Dotsch, Opt. Commun. 189 (2001) 251.
[21] M. Vanwolleghem, W.V. Parys, D.V. Thourhout, R. Baetds, F. Lelarge, G.O. Lafay, B. Thedrez, R.W. Speetjens, L. Lagae, Appl. Phys. Lett. 85 (2004) 3980.
[22] K. Xie, A.D. Boardman, M. Xie, Y.J. Yang, H.M. Jiang, H.J. Yang, G.J. Wen, J. Li, K. Chen, F.S. Chen, Opt. Commun. 281 (2008) 3275.
[23] K. Xie, H.M. Jiang, W.Y. Zeng, G.J. Wen, H.J. Yang, A.D. Boardman, M. Xie, Opt. Commun. 282 (2009) 3883.